SCIENTIFIC INSTRUMENT NEWS
2020 Vol. 15 SEPTEMBER
Technical magazine of Electron Microscope and Analytical Instruments.
Article

In situ Investigation of Reversible Exsolution/Dissolution of CoFe Nanoparticles in Perovskite

Lv Houfu
Ph.D.
Dalian Institute of Chemical Physics
Chinese Academy of Sciences

1. Introduction

Solid oxide fuel cells (SOFCs) and solid oxide electrolysis cells (SOECs) are electrochemical energy conversion devices that have demonstrated high energy conversion efficiency by high-temperature operation. Perovskite materials have been extensively investigated as electrode materials both for cathodes and anodes. *In situ* exsolving metal nanoparticles on the active metal doped perovskite through reduction atmosphere treatment to establish highly active metal-oxide interface is an effective way to enhance catalytic activity of the perovskites[1, 2]. The exsolved metal nanoparticles possess excellent operation stability by their socketed structure on the perovskite. Moreover, these exsolved metal nanoparticles can be "intelligent" catalyst, which means the metal-oxide interface can regenerate itself upon redox (reduction/oxidation) treatments. After operating for a long time, the metal nanoparticles may tend to coarsening, agglomeration or poisoning by the gaseous impurity such as sulfur or coking. Oxidant (air) will flush the sulfur or carbon species absorbed on the electrode, and the agglomerated metal nanoparticles could also be dissolved into the perovskite, the electrode can be regenerated again through a reductant (H_2) treatment to obtain elaborate metal nanoparticles again. Which can significantly alleviate the agglomeration of the metal nanoparticles and enhance the lifetime of the highly active metal-oxide interface catalyst[3, 4]. A redox stable electrode is a better choice both for SOFCs anodes and SOECs cathodes.

In the past decade, *in situ* exsolution strategy has been extensively exploited for perovskite-type (ABO_3) oxides due to their high structural stability in a redox treatment and allowing for almost all transition and rare earth metals in A or B sites. The successful construction of active perovskite supported metal or alloy nanoparticles ranges from noble metals (such as Pt, Pd, Rh, Ru, Ir and Ag) to transition metals (such as Fe, Co, Ni and Cu)[2]. Understanding and controlling the formation of nanoparticles on the surface of functional perovskite oxide supports is critical for tuning activity and stability for catalytic for energy conversion applications. *In situ* transmission electron microscopy (TEM) has been employed to provide insights at nanoscale into the exsolution of metallic nanoparticles in perovskites under reducing atmosphere[5-7]. Luo *et al*. used *in situ* TEM to investigate the exsolution of Co nanoparticles in $Pr_{0.5}Ba_{0.5}Mn_{0.9}Co_{0.1}O_3$ perovskite, provided a real time observation (dark field (DF) images) of the emergent process via an environmental transmission electron microscopy (ETEM)[5]. Kim *et al*. measured the growth kinetics of individual Co particles exsolved on $SrTi_{0.75}Co_{0.25}O_{3-\delta}$ polycrystalline thin films perovskite using *in situ* TEM[6]. They found that the exsolution of Co nanoparticles preferentially occurs at grain boundaries and corners which that are energetically favorable locations to minimize their nucleation energy barriers. Tsampas *et al*. used a latest generation *in situ* ETEM to follow the exsolution of individual nanoparticles at the surface of $La_{0.43}Ca_{0.37}Ni_{0.06}Ti_{0.94}O_3$ perovskite, with ultrahigh spatial and temporal resolution[7]. Whereas, except for the crystal reconstruction from the bulk phase information, three dimensional surface morphology evolution for the perovskite surface and topographical information reflecting the exsolved metal nanoparticles are very important to provide a deep understanding of the formation of the nanoparticles and demonstrate the tailoring of the nano-interfaces. Furthermore, the dissolution process and structural evolution under oxidizing atmosphere also deserve more detailed research to get fundamental understanding of the redox

reversibility in order to design highly efficient and regenerative metal-oxide interfaces. Therefore, an instrument with highly spatial resolution and high sensitivity TEM instrument equipped with highly sensitive secondary electron (SE) detector have extensive requirements and unlimited space. Hitachi HF5000 as an *in situ* scanning transmission electron microscopy (STEM) is therefore brought to our attention.

In consideration of economic feasibility, we focus on the study about redox reversible exsolution/dissolution of CoFe alloy nanoparticles in $Sr_2Fe_{1.35}Co_{0.2}Mo_{0.45}O_{6-\delta}$ (SFMC) and $La_{0.4}Sr_{0.6}Co_{0.2}Fe_{0.7}Mo_{0.1}O_{3-\delta}$ (LSCFM) perovskites, which are commonly used in SOFCs and SOECs as the redox stable and highly active electrode materials[8-11]. Metal oxide perovskites have the advantages of structural stability, even under high temperature (1300 °C) and a wide range of oxygen partial pressure. Taking advantage of the *in situ* atmosphere and high operation temperature, the surface and structural information from the SE, BF and DF-STEM images from Hitachi HF5000, we can obtain a direct geometrical structure and acquire a deep understanding of the behaviors under redox manipulations.

2. Overview and Specifications about Hitachi HF5000

Hitachi HF5000 field emission scanning transmission microscope (STEM) is an instrument equipped with cold field emission electron gun with an accelerating voltage of 200 kV (Figure 1). Meanwhile, the instrument is equipped with three STEM detectors: a bright field STEM (BF-STEM) detector and an annular dark field STEM (DF-STEM or HAADF-STEM) detector, and a secondary electron (SE) detector installed on the upper side above the objective lens. All three signals can be recorded and saved simultaneously, both as static images or as movies, atomic resolution images and movies can be obtained from room temperature to high temperature and *in situ* atmosphere conditions (20-1200 °C for the MEMS chip). An advantage of this measurement is that multiple types of information can be obtained at the same time: the DF-STEM image indicates atomic number dependent Z-contrast, the BF-STEM image indicates phase contrast, and the SE-STEM image reflects the three dimensional surface structure of the sample. An advantage of this measurement is the acquisition of atomic resolution DF, BF and SE images simultaneously[12]. As a highly spatial resolution and high sensitivity TEM/STEM instrument, HF5000 equipped with high atomic resolution energy dispersive X-ray spectroscopy (EDS) and electron energy loss spectrum (EELS), which makes it a powerful tool for a wide range of users.

In situ conditions: the experiment was performed using MEMS heating holder, and the gas flow was controlled by MFC systems (flow: 2 mL min^{-1} and pressure: ~10 Pa of pure H_2 or O_2). Our sample was supported on the 50 nm thick Si_3N_4 membrane, the gas was injected to the sample area directly by a special gas injection nozzle.

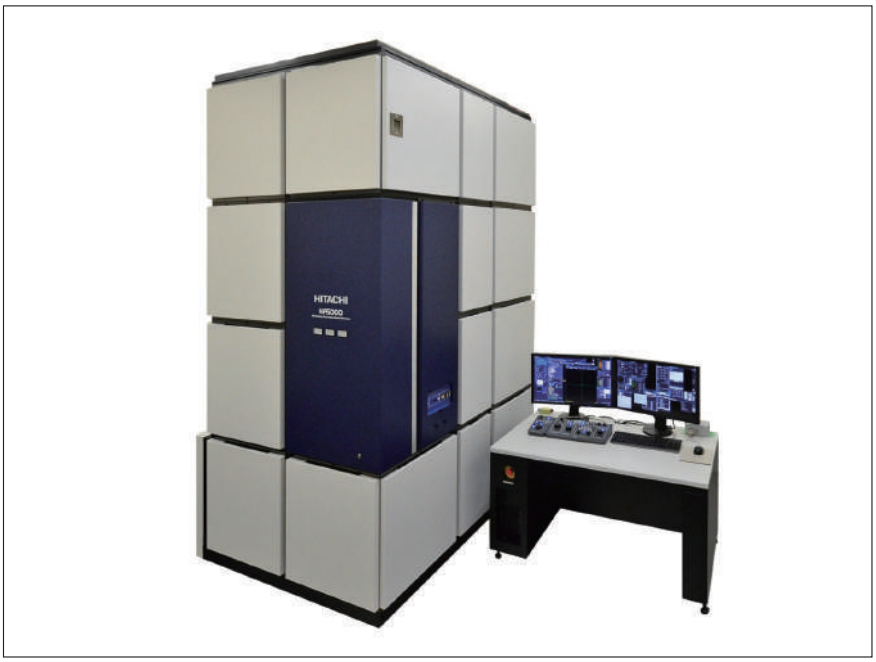

Fig. 1 Hitachi HF5000, *in situ* environmental aberration-corrected TEM/STEM/SE. Hitachi High-Technologies Corporation.

3. Illustrative Observations

Structurally, the A site cations in the perovskite are 12-fold coordinated lanthanide or alkali earth metal ions, while B site cations are 6-fold 3d transition metal ions coordinated with oxygen anions (Figure 2a). In reductive environment, exsolution begins with the oxygen escaping from the oxygen sites, the easier to be reduced B sites cations exsolved from bulk lattice, which is known as the co-segregation of cations with oxygen vacancies (Figure 2b). Subsequently, possible phase decomposition/transformation and surface reconstruction occur along with the exsolved metal nanoparticles. And after re-oxidation, nanoparticles can be dissolved back into the perovskite with the perovskite back to the original structure (Figure 2c). Such smart behavior opens the door to alleviate the poor stability and serious agglomeration problems for supported catalysts. It is worthy to take advantage of *in situ* instruments to have a deep insight into the exsolution/dissolution phenomena.

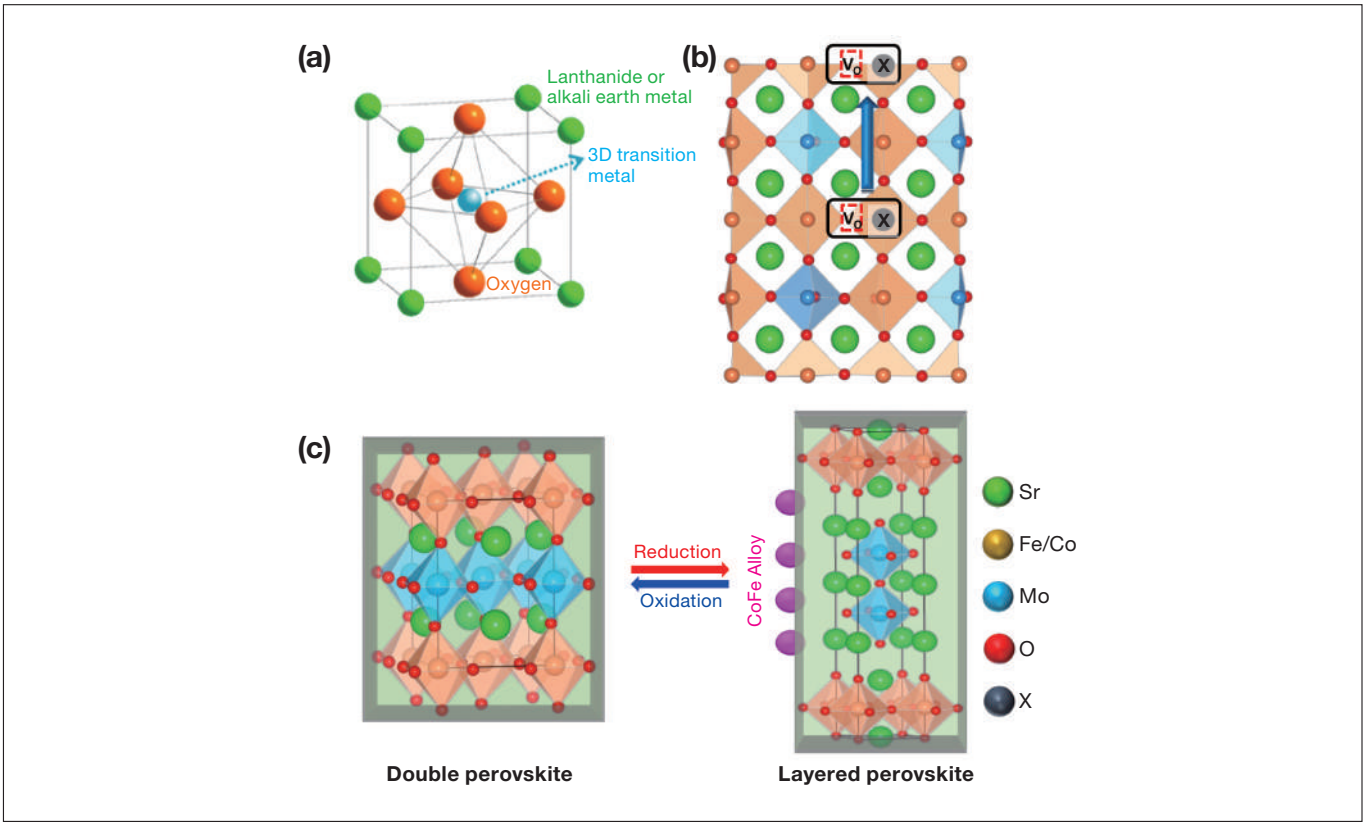

Fig. 2 (a) Illustration of crystal structure of ABO_3 perovskite oxides. Reproduced with permission[2]. Copyright 2020, American Chemical Society. (b) Schematic illustration of the model used to show the segregation of B sites caions. (V_O means oxygen vacancy. X denotes the dopants: iron, cobalt, and molybdenum atoms). (c) Schematic representation of the exsolution and dissolution process of B sites caions. Reproduced with permission[9]. Copyright 2020, Wiley.

3-1. *In situ* observation of surface morphology

We have used *in situ* STEM (HF5000) to provide direct insight into the exsolution/dissolution of CoFe alloy nanoparticles in SFMC perovskite under both reducing and oxidizing atmospheres[9]. In Figure 3a, CoFe alloy nanoparticles emerge during the reduction and then vanish during the re-oxidation at the same location. The local structure of the re-oxidized sample is essentially the same as that of the as-prepared sample, with no aggregation of CoFe alloy nanoparticles and alter surface roughness, demonstrating the self-regeneration functions. Figure 3b shows direct insights into emerging, growing (circled with a yellow full line), and coarsening (circled with a yellow dashed line) processes of CoFe alloy nanoparticles on the perovskite under H_2 atmosphere. We then focus on *in situ* observation of the re-oxidation process, which has seldom been reported in the literatures, especially from SE-STEM pictorial information. Figure 3c shows direct insights into the re-oxidation process. The CoFe alloy nanoparticles are oxidized fleetly to flaky particles that are attached onto the perovskite surface at 600 °C, and the flat oxide particles with irregular shape do not restore back to the parent perovskite until the temperature ascends to 800 °C. An obvious morphology change occurs during the inter-diffusion between the oxide nano-sheets and the perovskite.

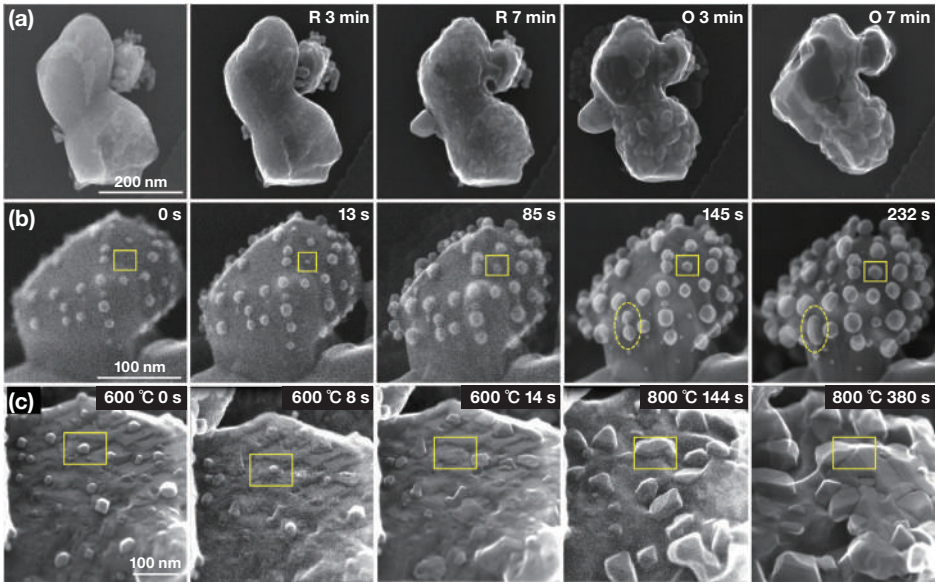

Fig. 3 ***In situ*** **STEM images of SFMC before reduction, after reduction, and re-oxidation. (a) Secondary electron microscopy images of a reduction/re-oxidation cycle at 800 °C; R means reduction, and O means oxidation. (b) Secondary electron microscopy images of a typical area in 10 Pa of H_2 supplied at 800 °C and (c) secondary electron microscopy images of a typical area with 10 Pa of O_2 supplied at 600 °C for 22 s, then increasing from 600 to 800 °C with a heating rate of 5 °C s^{-1} and then stay at 800 °C. Time begins after supplying O_2 toward the sample. Reproduced with permission[9]. Copyright 2020, Wiley.**

We also have success with another material: LSCFM perovskite. The exsolution and dissolution of CoFe alloy nanoparticles under reducing and oxidizing conditions was monitored *in situ* by HF5000 (Figure 4a-d). As-prepared LSCFM shows a glaze surface. SE images display that the nanoparticles begin to emerge after reduction at 600 °C, the nanoparticles were found to be exsolved preferentially at the boundaries of the perovskite. The particle size and density increase after reduction at 700 °C, especially at the grain boundaries, and the nanoparticles reincorporate back into the perovskite lattice after re-oxidation at 700 °C, demonstrating excellent redox recyclability of LSCFM. Except for the surface morphology evolution, elemental information were also obtained during the *in situ* exsolution (Figure 4e-h). DF-STEM images and elemental maps were collected during *in situ* exsolution, Co or Co-rich nanoparticles were exsolved after reduction at 600 °C (Figure 4f), while CoFe alloy nanoparticles were assembled after reduction at 700 °C (Figure 4h). So the *in situ* measurements by HF5000 visualized the sequential exsolution order of Co and Fe caions and formation of CoFe alloy nanoparticles, as well as reversible exsolution and dissolution of CoFe alloy nanoparticles in LSCFM.

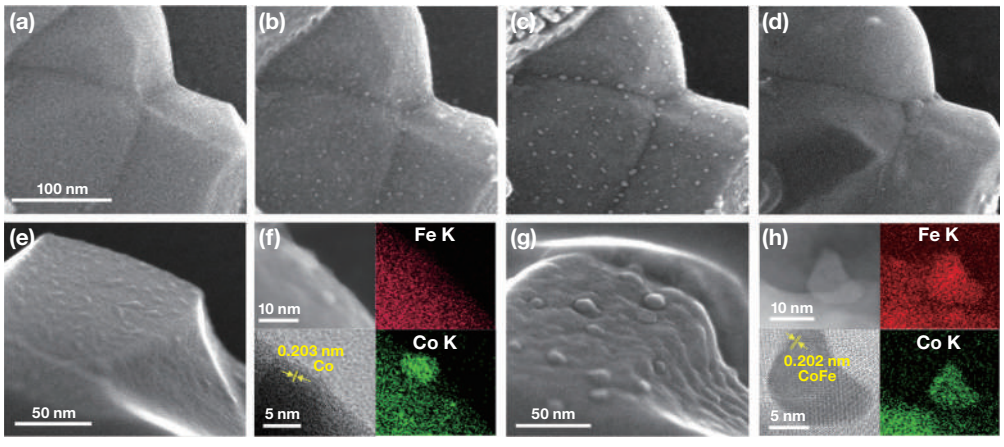

Fig. 4 ***In situ*** **SE-STEM images of LSCFM: (a) before reduction, (b) after reduction in 10 Pa of H_2 supplied at 600 °C, (c) after reduction in 10 Pa H_2 supplied at 700 °C and (d) after re-oxidation in 10 Pa O_2 supplied at 700 °C. (e, f) *In situ* SE, DF and BF-STEM images and the corresponding elemental maps of LSCFM after reduction at 600 °C. (g, h) *In situ* SE, DF and BF-STEM images and the corresponding elemental maps of LSCFM after reduction at 700 °C. Reproduced with permission[11]. Copyright 2020, Wiley.**

3-2. Atomic-scale analysis of the perovskite structure

Usually, metal oxide perovskites have a large particle size formed from the calcination under high temperature that is needed to form the perovskite structure (Figure 5a). The region needed for atomic-scale analysis needs to be thin enough for electron-transparent and preferably oriented along a major crystallographic axis. The thin area could be obtained through grinding or slicing up of the powders during the sample preparation. In the microscopy, the HF5000 incorporates the Cs corrector, which is very advantageous to find the appropriate areas. Figure 5b and 5c show the DF, BF, and SE-STEM images and atomic resolution STEM-EDS elemental maps of LSCFM. In the DF-STEM images, La and Sr atoms in the A sites of perovskite appear as bright spots due to their high atomic number (Z = 57 and 38), while the gray spots represent for Co, Fe and a spot of Mo atoms in the B sites of the LSCFM perovskite. The ability to observe atomic resolution SE images as shown in Figure 5b in real time is among the most powerful features of the HF5000. The atomic resolution EDS elemental maps further confirmed the distribution of each element, and the most important, we confirmed that the doped Mo element is deposited in the B sites of the perovskite clearly.

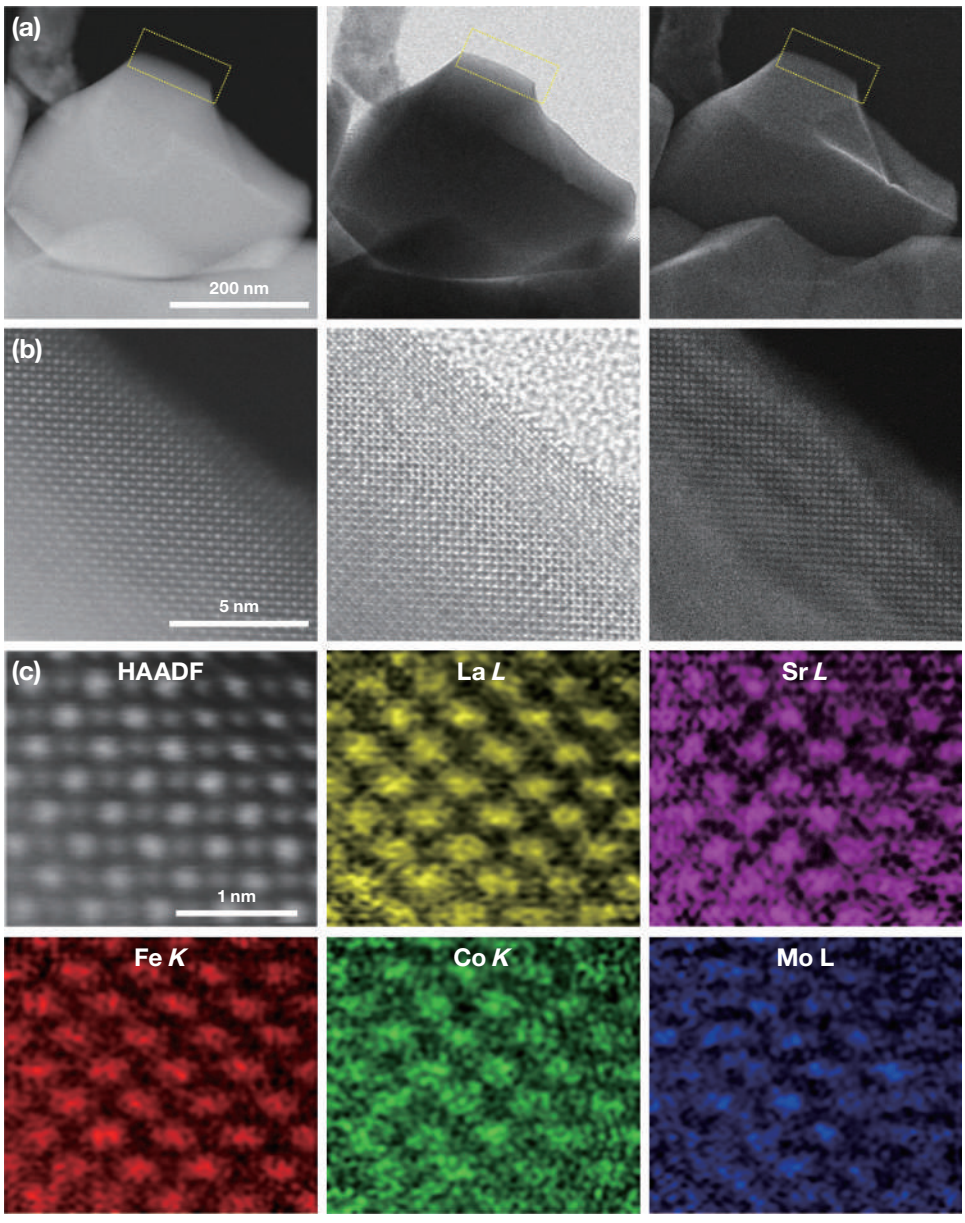

Fig. 5 Atomic-scale STEM results with STEM-EDS maps of LSCFM. (a, b) DF, BF, SE-STEM images of as-prepared LSCFM. (c) HAADF-STEM image and the corresponding elemental maps. The images were Wiener filtered. Reproduced with permission[11]. Copyright 2020, Wiley.

After reduction in H_2, a mount of CoFe alloy nanoparticles were exsolved on the surface of LSCFM. The exsolved CoFe alloy nanoparticles were attached on the parent perovskite (Figure 6a), indicating a strong interaction between the exsolved nanoparticle and the perovskite. Elemental maps were also performed to confirm the composition of the exsolved nanoparticle (Figure 6b), all the elements are evenly distributed in the substrate, whereas only Co and Fe could be seen in the nanoparticle, confirming the exsolution of CoFe alloy nanoparticles. Furthermore, the substrate perovskite was also characterized by the DF-STEM and elemental maps, the positions of La, Sr, Co, Fe and Mo remain unchanged (Figure 6c) compared with that before reduction (Figure 5b and 5c), indicating the stable perovskite under reducing atmosphere. Combine with the *in situ* results in Figure 4, we show another structural stable and redox renewable perovskite electrode.

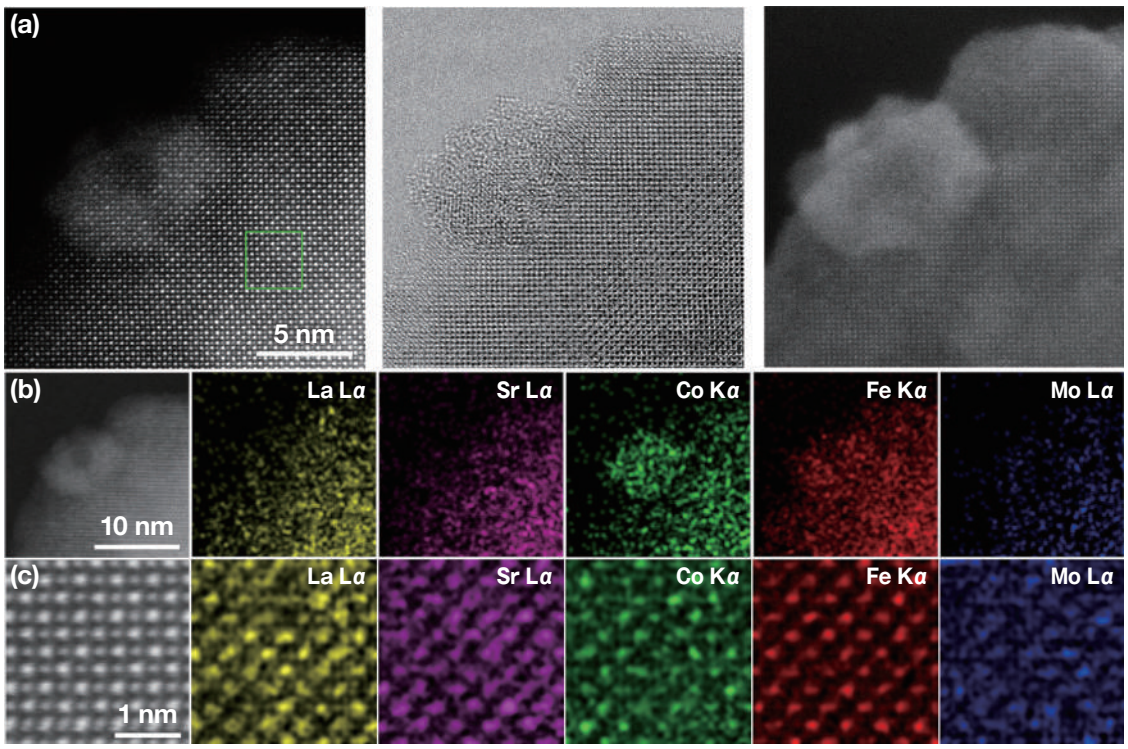

Fig. 6 Atomic-scale STEM results with STEM-EDS maps of LSCFM after reduction. (a) DF, BF, and SE-STEM images of LSCFM with an exsolved CoFe nanoparticle. (b) DF-STEM image and the corresponding STEM-EDS elemental maps. (c) Atomic-scale elemental maps of the parent perovskite, circled with a green full line in (a). The images were Wiener filtered. Reproduced with permission[11]. Copyright 2020, Wiley.

There have been a wide range applications of the emerging advanced HF5000. In the aspects of single-atoms catalysts[13, 14], intermetallic alloy catalyst[15], *et al*.

4. Conclusions

In this report, we presented the technological functions of Hitachi HF5000 (Environmental aberration-corrected TEM/STEM/SE) and our studies in the direct observation of nanoparticles exsolution/dissolution from the perovskites using HF5000. Expect for the *in situ* surface morphology evolution from the special SE-STEM images/videos, this instrument also offers ultrahigh spatial and temporal resolution for structural information and atomic scale element sensitive information. Which helps us get three dimensional surface information, bulk structure and element information simultaneously. HF5000 as an advanced instrument, can provide *in situ* and high resolution characterizations in many aspects from a wide range of research territory.

Acknowledgements

The author thanks Hitachi High-Technologies Corporation for providing Hitachi HF5000 (Environmental aberration-corrected TEM/STEM/SE) for *in situ* and *ex situ* STEM and EDS measurements. I would like to show my deeply grateful to Hiroaki Matsumoto for his exquisite workmanship.

References

1) D. Neagu, G. Tsekouras, D. N. Miller, H. Menard, J. T. S. Irvine, *In situ* growth of nanoparticles through control of non-stoichiometry, *Nat. Commun*., **5**, **916** (2013).

2) J. Zhang, M. -R. Gao, J. Luo, *In Situ* Exsolved Metal Nanoparticles: A Smart Approach for Optimization of Catalysts, *Chem. Mater*., **32**, **5424** (2020).

3) D. Neagu, T. S. Oh, D. N. Miller, H. Menard, S. M. Bukhari, S. R. Gamble, R. J. Gorte, J. M. Vohs, J. T. S. Irvine, Nano-socketed nickel particles with enhanced coking resistance grown *in situ* by redox exsolution, *Nat. Commun*., **6**, **8120** (2015).

4) W. Wang, L. Gan, J. P. Lemmon, F. Chen, J. T. S. Irvine, K. Xie, Enhanced carbon dioxide electrolysis at redox manipulated interfaces, *Nat. Commun*., **10**, **1550** (2019).

5) Y. Sun, Y. Zhang, J. Chen, J. Li, Y. Zhu, Y. Zeng, B. S. Amirkhiz, J. Li, B. Hua, J. Luo, New Opportunity for *in Situ* Exsolution of Metallic Nanoparticles on Perovskite Parent, *Nano Lett*., **16**, **5303** (2016).

6) Y. R. Jo, B. Koo, M. J. Seo, J. K. Kim, S. Lee, K. Kim, J. W. Han, W. Jung, B. J. Kim, Growth Kinetics of Individual Co Particles Ex-solved on $SrTi_{0.75}Co_{0.25}O_{3-\delta}$ Polycrystalline Perovskite Thin Films, *J. Am. Chem. Soc*., **141**, **6690** (2019).

7) D. Neagu, V. Kyriakou, I. L. Roiban, M. Aouine, C. Tang, A. Caravaca, K. Kousi, I. Schreur-Piet, I. S. Metcalfe, P. Vernoux, M. C. M. van de Sanden, M. N. Tsampas, *In Situ* Observation of Nanoparticle Exsolution from Perovskite Oxides: From Atomic Scale Mechanistic Insight to Nanostructure Tailoring, *ACS Nano*, **13**, **12996** (2019).

8) Q. Liu, X. Dong, G. Xiao, F. Zhao, F. Chen, A novel electrode material for symmetrical SOFCs, *Adv. Mater*., **22**, **5478** (2010).

9) H. Lv, L. Lin, X. Zhang, Y. Song, H. Matsumoto, C. Zeng, N. Ta, W. Liu, D. Gao, G. Wang, X. Bao, *In Situ* Investigation of Reversible Exsolution/Dissolution of CoFe Alloy Nanoparticles in a Co-Doped $Sr_2Fe_{1.5}Mo_{0.5}O_{6-\delta}$ Cathode for CO_2 Electrolysis, *Adv. Mater*., **32**, **1906193** (2020).

10) W. Zhang, H. Wang, K. Guan, J. Meng, Z. Wei, X. Liu, J. Meng, Enhanced Anode Performance and Coking Resistance by *In Situ* Exsolved Multiple-Twinned Co-Fe Nanoparticles for Solid Oxide Fuel Cells, *ACS Appl Mater Interfaces*, **12**, **461** (2020).

11) H. Lv, T. Liu, X. Zhang, Y. Song, H. Matsumoto, N. Ta, C. Zeng, G. Wang, X. Bao, Atomic-Scale Insight into Exsolution of CoFe Alloy Nanoparticles in $La_{0.4}Sr_{0.6}Co_{0.2}Fe_{0.7}Mo_{0.1}O_{3-\delta}$ with Efficient CO_2 Electrolysis, *Angew. Chem. Int. Ed*., DOI: 10.1002/anie.202006536 (2020).

12) H. Inada in the Volume 11, "HF5000 Field-emission Transmission Electron Microscope: High Spatial Resolution and Analytical Capabilities for Material Science", *Hitachi Scientific Instrument News* (2018).

13) K. Liu, X. Zhao, G. Ren, T. Yang, Y. Ren, A.F. Lee, Y. Su, X. Pan, J. Zhang, Z. Chen, J. Yang, X. Liu, T. Zhou, W. Xi, J. Luo, C. Zeng, H. Matsumoto, W. Liu, Q. Jiang, K. Wilson, A. Wang, B. Qiao, W. Li, T. Zhang, Strong metal-support interaction promoted scalable production of thermally stable single-atom catalysts, *Nat. Commun*., **11**, **1263** (2020).

14) B. Han, T. Li, J. Zhang, C. Zeng, H. Matsumoto, Y. Su, B. Qiao, T. Zhang, A highly active Rh/CeO_2 single-atom catalyst for low-temperature CO oxidation, *Chem. Commun*., **56**, **4870** (2020).

15) X. Zhang, S. Han, B. Zhu, G. Zhang, X. Li, Y. Gao, Z. Wu, B. Yang, Y. Liu, W. Baaziz, O. Ersen, M. Gu, J. T. Miller, W. Liu, Reversible loss of core-shell structure for Ni-Au bimetallic nanoparticles during CO_2 hydrogenation, *Nature Catalysis*, **3**, **411** (2020).